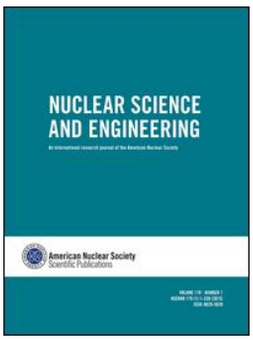

Nuclear Science and Engineering

ISSN: 0029-5639 (Print) 1943-748X (Online) Journal homepage: http://www.tandfonline.com/loi/unse20

Neutron Displacement Cross Sections for Stainless Steel and Tantalum Based on a Lindhard Model

D.G. Doran

To cite this article: D.G. Doran (1972) Neutron Displacement Cross Sections for Stainless Steel and Tantalum Based on a Lindhard Model, Nuclear Science and Engineering, 49:2, 130-144, DOI: 10.13182/NSE72-A35501

To link to this article: http://dx.doi.org/10.13182/NSE72-A35501

Published online: 12 May 2017.

NUCLEAR SCIENCE AND ENGINEERING: 49, 130-144 (1972)

Neutron Displacement Cross Sections for Stainless Steel and Tantalum Based on a Lindhard Model

D. G. Doran

Hanford Engineering Development Laboratory, Westinghouse Hanford Company
P. O. Box 1970, Richland, Washington 99352

Received November 8, 1971
Revised April 14, 1972

The theory developed by Lindhard and co-workers for the partition of energy as an energetic ion slowing down in a solid has been applied to the calculation of neutron displacement cross sections for iron, chromium, nickel, stainless steel, and tantalum. ENDF/B data were used to incorporate anisotropic elastic and isotropic inelastic neutron scattering. A contribution from (n,γ) recoils has also been included. The results for stainless steel are presented in tabular form for convenience.

INTRODUCTION

Energy dependent neutron displacement cross sections have been computed for stainless steel and tantalum based on the theory of slowing down of energetic atoms in solids due to Lindhard et al.[1] They were developed to fill several needs. An absolute measure of damaging radiation dose is required to correlate experimental results obtained in different neutron spectra and by ion bombardment.[2,3] On the other hand, a relative measure of the energy dependence of damage (defined here as any property change resulting from radiation-induced displacements) is employed as a starting function in the iterative procedure used to determine an empirical damage cross section.[4] If the empirical work is to increase our understanding of damage mechanisms, it is vital to have a model-based damage cross section for comparison with the empirically determined one. In modeling radiation damage, furthermore, it is necessary to estimate the production rates of free and bound defects—the displacement cross section is the logical starting point.

Available displacement cross sections for iron are considered deficient because either they are based on the Kinchin-Pease model for displacement efficiency per knock-on atom,[5,6] or do not include the contribution from inelastic scattering of neutrons.[7] Knock-on atoms produced by fast neutrons are sufficiently energetic that appreciable energy is lost to electrons. The Kinchin-Pease model accounts for such loss only by designating a threshold energy above which all energy loss is by ionization (no displacements) and below which all energy loss results in displacements. The Lindhard model is a more realistic treatment of ionization losses. It has been used previously to compute displacement rates by heavy-ion bombardment,[2,3] and has also been employed in neutron irradiation damage analyses.[8,9]

[1] J. LINDHARD, V. NIELSEN, M. SCHARFF, and P. V. THOMSEN, *Mat. Fys. Medd. Dan. Vid. Selsk.*, **33**, No. 10 (1963).

[2] G. L. KULCINSKI, J. J. LAIDLER, and D. G. DORAN, *Rad. Effects*, **7**, 195 (1971).

[3] D. G. DORAN and G. L. KULCINSKI, *Rad. Effects*, **9**, 283 (1971).

[4] W. N. McELROY, R. E. DAHL, Jr., and C. Z. SERPAN, Jr., *Nucl. Appl. Tech.*, **7**, 561 (1969).

[5] J. D. JENKINS, *Nucl. Sci. Eng.*, **41**, 155 (1970).

[6] W. F. SHEELY, *Nucl. Sci. Eng.*, **29**, 165 (1967).

[7] G. E. RUSSCHER, "Calculated Damage Functions for Determining Irradiation Effectiveness," BNWL-1093, Battelle-Northwest Laboratories (1969).

[8] M. T. ROBINSON, "The Energy Dependence of Neutron Radiation Damage in Solids," in *Proc. Nuclear Fusion Reactors Conf.*, p. 364, British Nuclear Energy Society, Culham Laboratory (September 1969).

[9] G. R. PIERCY, *J. Nucl. Mat.*, **29**, 267 (1969).

On the other hand, inelastic scattering of neutrons becomes significant in the MeV range in which many neutrons are found in fast reactors and hence cannot be neglected.

Lindhard et al. have derived from Thomas-Fermi theory a function $L(\epsilon)$ which is the kinetic energy, in dimensionless form, that is transferred to the atoms of a cascade initiated by a primary knock-on atom (PKA) having initial dimensionless energy ϵ. That is, the fraction of PKA energy available to cause displacements is $L(\epsilon)/\epsilon$; the remainder is lost in electron excitation. In the present work, the number of displacements per PKA is taken to be

$$\nu(T) = \frac{L(\epsilon)}{\epsilon}\frac{T}{2E_d} \quad , \tag{1a}$$

where T is the kinetic energy of the PKA in the laboratory system, $\epsilon = A_L T$, and E_d is an effective displacement energy. The characteristic energy A_L^{-1} is defined by

$$A_L = \frac{0.8853\, A_2}{(27.2)\, Z_1 Z_2 (Z_1^{2/3} + Z_2^{2/3})^{1/2} (A_1 + A_2)} \text{ eV}^{-1} \quad , \tag{1b}$$

where A_1 and Z_1 are atomic weight and number of the moving particle and A_2 and Z_2 are like quantities for the matrix atoms. The expression for $L(\epsilon)$ due to Robinson[8] was used for convenience:

$$L(\epsilon) = \epsilon\,[1 + k_L g(\epsilon)]^{-1} \tag{1c}$$

$$g(\epsilon) = \epsilon + 0.40244\, \epsilon^{3/4} + 3.4008\, \epsilon^{1/6} \tag{1d}$$

$$k_L = \frac{(0.0793)\, Z_1^{2/3}\, Z_2^{1/2} (A_1 + A_2)^{3/2}}{(Z_1^{2/3} + Z_2^{2/3})^{3/4}\, A_1^{3/2}\, A_2^{1/2}}$$

(from Lindhard[1]) . (1e)

For the case of a single constituent rather than an alloy, $A_1 = A_2 = A$, $Z_1 = Z_2 = Z$, and the expressions for A_L and k_L simplify to

$$A_L = 0.01151/(Z)^{7/3}\ \text{eV}^{-1},\quad k_L = 0.1334(Z)^{2/3}/(A)^{1/2} \, . \tag{1f}$$

Use of Eq. (1f) for pure iron, chromium, or nickel gives results differing by less than 1% from the results obtained by using Eqs. (1b) and (1e) for these metals as constituents of stainless steel.

The use of Eq. (1f) requires some justification. This particular form is used because Robinson[10] and Sigmund[11] have shown that, for elastic scattering of atoms, $\nu(T)$ can generally be expressed as

$$\nu(T) = \beta T/2E_d \quad , \tag{2}$$

where the displacement efficiency β is not much different from unity. It should be noted that the displacement efficiency determined in Beeler's[12] computer experiments (extending to 20 keV) was not constant, but decreased slightly with increasing PKA energy. Torrens and Robinson,[13] on the other hand, have found a constant efficiency for PKA energies up to 100 keV in initial computer experiments with a new cascade simulation code.

Accurate effective values of E_d are not known (see Appendix), so the value of the factor β/E_d has been chosen to be consistent with the computer experiments of Beeler.[12] For stainless steel, a value of 33 eV was used for E_d to give agreement with Beeler's work on α-iron at low PKA energy. For tantalum, a value of 68 eV was used to give agreement with Beeler's work on tungsten, reduced by the ratio of the cohesive energies of tantalum and tungsten. Neither value of E_d can be considered to have an accuracy of better than perhaps 30%. The final displacement cross sections are inversely proportional to E_d and hence can be easily altered for different values of E_d.[14]

The general expression for the displacement cross section per atom per unit fluence evaluated at a neutron energy E is

$$F(E) = \sigma(E) \int_{E_d}^{T^{\max}} \left[\frac{1}{\sigma}\frac{d\sigma(E,\phi)}{d\Omega}\right] \frac{d\Omega}{dT}(E,\phi)\, \nu(T)\, dT \quad , \tag{3}$$

where $\sigma(E)$ is an appropriate interaction cross section, $d\Omega$ an element of solid angle, ϕ the scattering angle in the center-of-mass (CM) system, and $T^{\max} = \gamma E$, the maximum possible PKA energy corresponding to a head-on collision ($\phi = 180°$). The constant γ is defined below Eq. (4).

A general expression relating T, E, ϕ and E_m, the energy of the scattered neutron in the CM system, is found from conservation of momentum to be

$$T = \eta_1\eta_2 E + (\eta_1/\eta_2)E_m - 2\eta_1 (EE_m)^{1/2} \cos\phi \quad , \tag{4}$$

where

$$\eta_1 = 1.009/(1.009 + A_2)$$

$$\eta_2 = A_2/(1.009 + A_2)$$

and

$$\gamma = 4\eta_1\eta_2 \, .$$

[10] M. T. ROBINSON, *Phil. Mag.*, **17**, 639 (1968).

[11] P. SIGMUND, *Rad. Effects*, **1**, 15 (1969).

[12] J. R. BEELER, Jr., *Phys. Rev.*, **150**, 470 (1966).

[13] I. M. TORRENS and M. T. ROBINSON, "Computer Simulation of Atomic Displacement Cascades in Solids," *Interatomic Potentials and Simulation of Lattice Defects*, P. C. GEHLEN, J. R. BEELER, Jr., and R. I. JAFFEE, Eds., p. 423, Plenum Press, New York (1972).

[14] This statement is true to a very high approximation except for energies only slightly exceeding E_d.

Equation (3) was evaluated for both elastic and inelastic neutron scattering. The principal source of scattering cross section data was the Evaluated Nuclear Data File (ENDF/B-II);[15] BNL-325 was used in the resonance regions for chromium, nickel, and tantalum where pointwise data were not tabulated (below 0.65, 0.65, and 0.1 MeV, respectively). Some angular distribution data for chromium and nickel were taken from the third edition of BNL-400.

ELASTIC SCATTERING

For elastic scattering, energy conservation gives $E_m = \eta_2^2 E$ and Eq. (4) becomes

$$T = (\tfrac{1}{2})\gamma E(1 - \cos\phi) \qquad (5)$$

and therefore

$$d\Omega/dT = -2\pi\, d\cos\phi/dT = 4\pi/\gamma E = 4\pi/T^{\max} \quad . \qquad (6)$$

Elastic scattering at low energies ($<\sim$0.1 MeV for iron, nickel, and chromium; $<\sim$0.05 MeV for tantalum) is sufficiently isotropic that

$$d\sigma(E,\phi)/d\Omega = \sigma(E)/4\pi \quad . \qquad (7)$$

For higher energies, available data on angular distributions permit the calculation of $F(E)/\sigma(E)$ at a number of energies.

It is convenient to rewrite Eq. (3) in terms of $\mu = \cos\phi$. Let $p(E,\mu)$ be the probability that a neutron of energy E is scattered at the angle $\cos^{-1}\mu$. Then

$$p(E,\mu) \equiv \frac{2\pi}{\sigma(E)}\frac{d\sigma}{d\Omega}(E,\mu) \quad ,$$

and Eq. (3) becomes

$$\begin{aligned} R(E) &\equiv \left.\frac{F(E)}{\sigma(E)}\right|_{\text{elastic}} \\ &= \frac{4\pi}{T^{\max}}\int_{E_d}^{T^{\max}}\left[\frac{1}{\sigma}\frac{d\sigma}{d\Omega}(E,T)\right]\nu(T)\,dT \\ &= \int_{-1}^{1-r} p(E,\mu)\,\nu[T(E,\mu)]\,d\mu \quad , \end{aligned} \qquad (8)$$

where $r \equiv 2E_d/T^{\max}$. Except for energies very close to the displacement threshold, $r = 0$ is a legitimate approximation. A computer program was written to evaluate Eq. (8) using either pointwise data or a Legendre polynomial representation of $P(E,\mu)$.

The function $R(E)$, which is just the mean number of displacements per PKA, was interpolated to convert the elastic scattering cross section data (generally much more abundant than angular distribution data) to the desired displacement cross section. Plots of $R(E)$ are presented in Fig. 1 for iron, chromium, and nickel and in Fig. 2 for tantalum. The function $R(E)$, as well as the scattering and displacement cross sections, was reduced to a standard 621 group (10^{-10} - 18 MeV) structure consisting of 45 equal lethargy groups below 1 MeV, and 0.1 MeV groups above 1 MeV.

INELASTIC SCATTERING

General

For energies not greatly exceeding the inelastic scattering (n,n') threshold, the n,n' contribution to the displacement cross section can be obtained as a sum of contributions from resolved nuclear energy levels Q_i (taken positive here). Because the energy values at which cross section data are given do not generally coincide with energy values for which secondary neutron emission data are given, a function $R_i(E)$ was computed for each level. The contribution from resolved levels to the displacement cross section is then

$$F(E)\Big|_{\substack{\text{inelastic}\\ \text{resolved}}} = \sum_i R_i(E)\,\sigma_i^{in}(E) \quad , \qquad (9)$$

where $\sigma_i^{in}(E)$ is the partial n,n' cross section for the i'th level.

Energy conservation for an n,n' event yields

$$E_m = \eta_2(\eta_2 E - Q_i) \quad , \qquad (10)$$

which, when substituted into Eq. (4), gives

$$T_i = 0.5\,\gamma\{E - \mu[E(E - Q_i/\eta_2)]^{1/2}\} - Q_i\eta_1 \quad . \qquad (11)$$

From Eq. (11)

$$d\Omega/dT = 4\pi/\gamma[E(E - Q_i/\eta_2)]^{1/2} \quad . \qquad (12)$$

The upper (T^+) and lower (T^-) limits of the integral in Eq. (3) are given by $\mu = -1$ and $\mu = 1$,[16] respectively, in Eq. (11). Therefore

$$\begin{aligned} R_i(E)\Big|_{\substack{\text{inelastic}\\ \text{resolved}}} &= \frac{2}{\gamma[E(E - Q_i/\eta_2)]^{1/2}} \\ &\quad \times \int_{T_i^-}^{T_i^+} p_i[E,\mu(E,T)]\,\nu(T)\,dT \quad . \end{aligned} \qquad (13)$$

This can also be expressed as in Eq. (8):

$$R_i(E)\Big|_{\substack{\text{inelastic}\\ \text{resolved}}} = \int_{-1}^{1} p_i(E,\mu)\,\nu[T(E,\mu)]\,d\mu \quad . \qquad (14)$$

At high neutron energies, the inelastic scattering is described by an evaporation model characterized by an effective evaporation temperature

[15] Chromium, MAT 1121; Nickel, MAT 1123; Tantalum, MAT 1035. The iron data (MAT 1124, in the version published in Ref. 18) were kindly supplied in pointwise form by the Radiation Shielding Information Center at Oak Ridge National Laboratory.

[16] For sufficiently high E and low Q_i, $T^- < E_d$ is possible for $\mu > 1 - \epsilon$; ϵ is so small, however, that such a case is of no consequence.

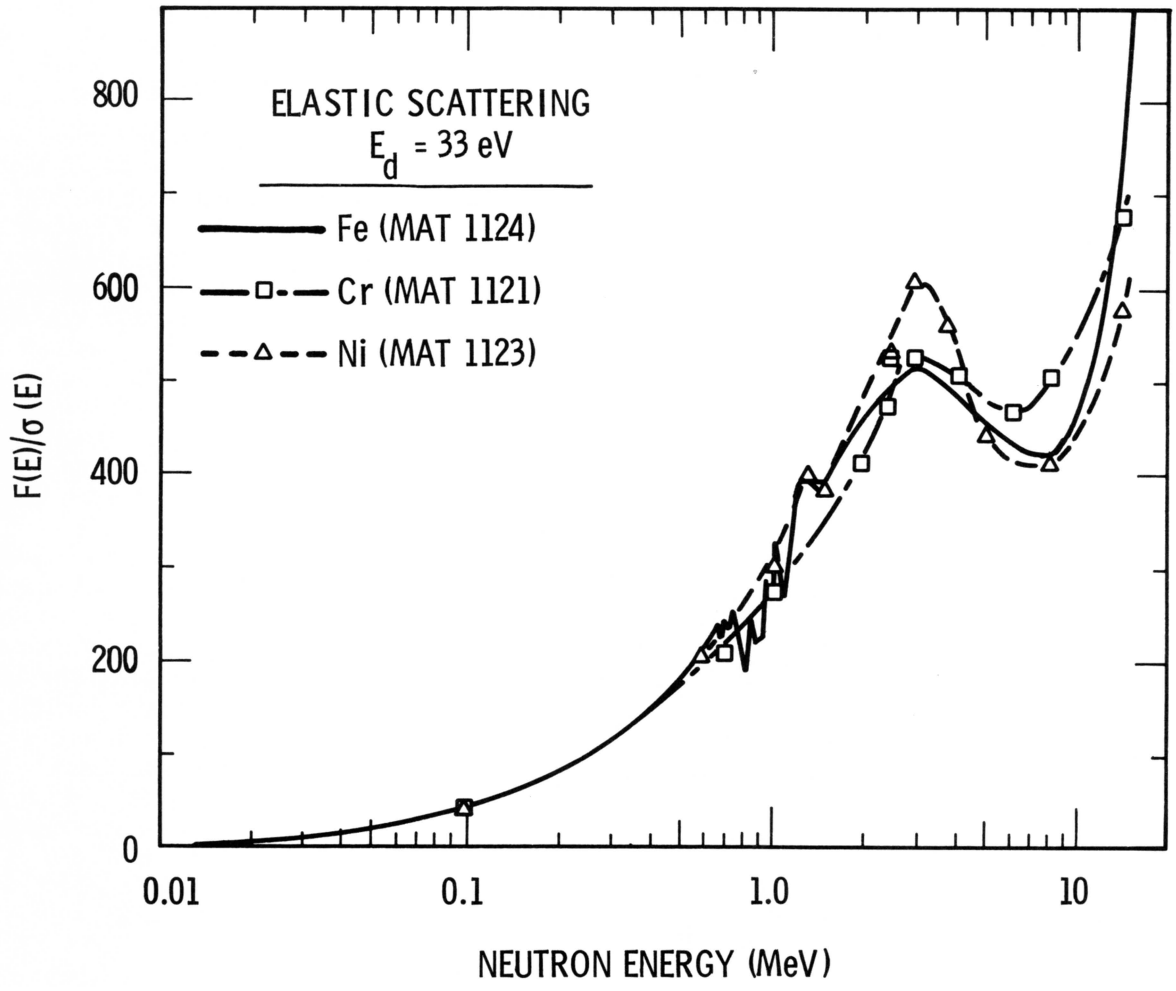

Fig. 1. The ratio of the elastic displacement cross section to the elastic scattering cross section, i.e., the mean number, $\bar{\nu}$, of displacements per PKA as a function of neutron energy for iron, chromium, and nickel.

$\Theta(E)$. In this model, the energy E_m of the scattered neutron (CM system) is distributed as[17]

$$f(E,E_m) = \frac{E_m}{I(E,\Theta)} \exp(-E_m/\Theta) \quad , \qquad (15)$$

where

$$I(E,\Theta) = \Theta^2[1 - (1 + E_m^{max}/\Theta)\exp(-E_m^{max}/\Theta)] \qquad (16)$$

is a normalization factor such that

$$\int_0^{E_m^{max}} f(E,E_m)\, dE_m = 1 \quad .$$

If the evaporation model replaces the discrete formulation at high energies, the maximum value

[17] Technically, Eq. (15) describes the distribution of the available energy in the CM system, $\eta_2 E = Q = E_m/\eta_2$. But $\eta_2 = 0.98$ for iron and 0.995 for tantalum, so $\eta_2 E = Q \cong E_m$. On the other hand, the ENDF/B parameters are for the laboratory system. The mean energy of the scattered neutron in the laboratory system is $E_m + \eta_1^2 E \cong E_m$ to a very good approximation except for E only slightly exceeding Q.

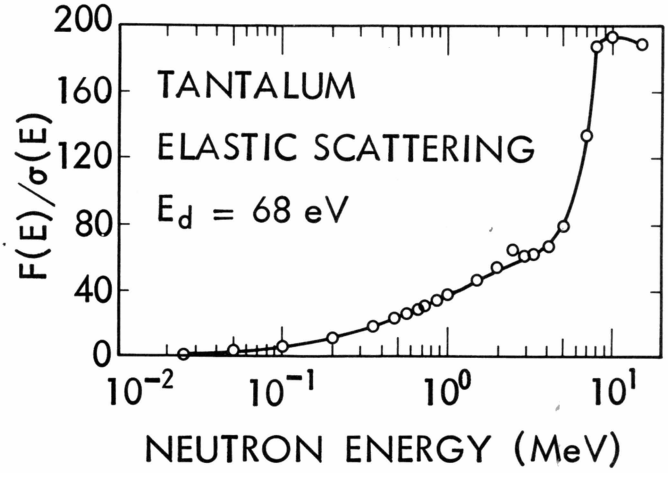

Fig. 2. The ratio of the elastic displacement cross section to the elastic scattering cross section, i.e., the mean number, $\bar{\nu}$, of displacements per PKA as a function of neutron energy for tantalum.

of E_m is given by Eq. (10) with $Q_i = Q_1$, the lowest energy level. However, the effective Q value is sometimes treated as an adjustable parameter to fix the maximum value of E_m. The minimum value of E_m is zero. For each value of E_m there is a range of values of T given by Eq. (4) as cos ϕ varies from 1 to -1. The upper and lower limits are then

$$T^{\pm} = \eta_1\eta_2 E + (\eta_1/\eta_2) E_m \pm 2\eta_1(EE_m)^{1/2} \quad (17)$$

and

$$\frac{d\Omega}{dT} = -2\pi\, d\cos\phi/dT = \pi/\eta_1(EE_m)^{1/2} \quad . \quad (18)$$

Assuming the angular distribution is isotropic, Eq. (3) becomes

$$F(E)\Big|_{\substack{\text{inelastic}\\ \text{continuum}}} = \sigma^{in}(E) \int_0^{E_m^{max}(E)} \int_{T^-(E_m)}^{T^+(E_m)} f(E,E_m) \times \frac{\nu(T)}{4\eta_1(EE_m)^{1/2}}\, dT\, dE_m \quad (19)$$

$$= \frac{\sigma^{in}(E)}{2} \int_0^{E_m^{max}(E)} \int_{-1}^{1} f(E,E_m) \times \nu[T(E,E_m,\mu)]\, d\mu\, dE_m \quad . \quad (20)$$

A computer program was written to evaluate Eqs. (14) and (20).

Iron

The description[18] of inelastic scattering for iron (Mat. 1124) is more complex than for the other metals considered here. For excitation energies in the range 0.9 to 4 MeV, a formulation embracing 20 resolved levels is used. Between 4 and 7 MeV the energy distribution of the emitted neutron is given in tabular form, $g(E_m)$, and above 7 MeV an evaporation model, $h(E_m)$, is used also. A weighting function, $w(E)$, is employed such that $f(E,E_m)$ in Eq. (19) is replaced by either $(1 - w)h$ or wg; $w(E)$ decreases from unity at 7 MeV to nearly zero at 15 MeV.

Chromium, Nickel, and Tantalum

The ENDF/B-II descriptions of inelastic scattering in chromium, nickel, and tantalum are in terms of resolved levels for energies below 3.3, 4.2, and 1.5 MeV, respectively; the evaporation (Maxwellian) model is used at higher energies. At the interface between the two descriptions, the displacement cross section was found to be discontinuous; in each case the discrete model gave the higher value—by 8, 6, and 26% for chromium, nickel, and tantalum. In smoothing the data, the discrete description was favored.

$n,2n$ REACTIONS

The threshold energies for $n,2n$ reactions in iron, chromium, and nickel are 11-12 MeV and the $n,2n$ cross section is less than the n,n' cross section at 14 MeV. Tantalum, on the other hand, has a threshold of ~8 MeV and at 14 MeV the $n,2n$ cross section is six times the n,n' cross section. The simplest way to include the $n,2n$ contribution is to add the $n,2n$ and n,n' cross sections. Two other approaches were investigated for iron and tantalum—a one-neutron model and a two-neutron model. The 1-n model differed from the n,n' treatment only in that E_m^{max} was determined from Eq. (10) with Q_1 replaced by the $n,2n$ threshold energy.[19]

The 2-n model is based on Odette's[20] modification of the sequential emission formulation of Segev.[21] A second neutron can be emitted only if the residual excitation of the nucleus after emission of the first neutron exceeds the binding energy of a neutron in the mass A nuclide. For the present application, the recoil energy after emission of the first neutron was taken to be the average value [cos $\phi = 0$ in Eq. (4)]. An approximate expression for the displacement cross section due to $n,2n$ processes is then:

$$F(E)\Big|_{n,2n} = \int_0^{E-U} \frac{E_m}{I(E)} \exp[-E_m/\Theta(E)] \times \int_0^{E-U-E_m} \frac{E'_m}{I(E,E_m)} \exp[-E'_m/\Theta(E)] \times \int_{-1}^{+1} \tfrac{1}{2}\nu[T(E,E_m,E'_m,\mu)]\, d\mu\, dE'_m\, dE_m \quad . \quad (21)$$

No distinction has been maintained between the CM and LAB systems, nor between $\Theta(E)$ of nuclide $A + 1$ and $\Theta(E)$ of nuclide A. The permissible energies (E'_m) for the second emitted neutron depend on the energy (E_m) of the first emitted neutron. The normalization factor $I(E)$ is as given in Eq. (16) with $E_m^{max} = E - U$; likewise $I(E,E_m)$ is Eq. (16) with E_m^{max} replaced by $E_m'^{max} = E - U - E_m$. The function $\nu(T)$ is again given by

[18] S. K. PENNY and W. E. KINNEY, "A Re-Evaluation of Natural Iron Neutron and Gamma-Ray Production Cross Sections—ENDF/B Material 1124," ORNL-4617, Oak Ridge National Laboratory (1971).

[19] This differs from the ENDF/B formulation in which the maximum energy of the emitted neutron is given as $E - U$ with $U = 0$ for the $n,2n$ case. For tantalum, the difference in $F(E)|_{n,2n}$ between using $U = 0$ and $U = 7.6$ MeV is 10% at 8 MeV, decreasing to <1% above 11 MeV.

[20] G. R. ODETTE, *Trans. Am. Nucl. Soc.*, **15**, 464 (1972).

[21] M. SEGEV, "Inelastic Matrices in Multigroup Calculations," ANL-7710, p. 374, Argonne National Laboratory (1971).

Eq. (1) and T can be expressed as

$$T = \frac{A}{A-1}\frac{\eta_1}{\eta_2}E'_m + \frac{A-1}{A}\overline{T}_1 - 2\left(\frac{\eta_1}{\eta_2}\right)^{1/2}(\overline{T}_1 E'_m)^{1/2}\mu \quad , \tag{22}$$

where $\overline{T}_1 = \eta_1\eta_2 E + (\eta_1/\eta_2)E_m$ is the mean recoil energy after emission of the first neutron.

The $n,2n$ contributions to the displacement cross sections for iron and tantalum calculated by the three approaches are compared in Table I. The maximum difference is only 5%.[22]

ABSORPTION (n,γ) REACTIONS

Many neutron spectra encountered in studies related to the development of fast breeder reactors have a significant soft component. Hence, it may be important for a displacement cross section to include the effect of recoil atoms produced by the emission of energetic gammas in n,γ reactions. The recoil energy is given in terms of the gamma-ray energy E_γ and the mass M of the recoiling atom by

$$T = E_\gamma^2/2\,Mc^2$$

or

$$T(\text{eV}) = [E_\gamma(\text{MeV})]^2/1.862\times 10^{-3}(A+1) \quad .$$

Mean recoil energies (see Table II) were derived from a recent compilation of gamma-ray spectra by Orphan, Rasmussen, and Harper.[23] The n,γ contribution to the displacement cross section was estimated by assuming these recoil energies to be independent of the energy of the incident neutron. Cross sections appropriate at thermal energy (0.0253 eV) are included in Table II.

TABLE II

Displacements from n,γ Reactions

Metal	Mean Recoil Energy (eV)	Displacements / Capture	E_n = 0.0253 eV: $\sigma_{n,\gamma}$ (b)	E_n = 0.0253 eV: Displacements / Atom-ϕt (b)
Fe	516	6.7	2.55	17
Cr	636	8.2	3.1	26
Ni	522	6.8	4.6	31
18/10 SS[a]				20
Ta	106	0.05	20.7	1

[a]Stainless steel of composition 72% Fe, 18% Cr, 10% Ni.

RESULTS AND DISCUSSION

The displacement cross sections, excluding the n,γ recoil contributions, are presented in Figs. 3 through 6 for iron, chromium, nickel, and tantalum. The $n,2n$ contributions were calculated with the 2-n model. The combined contributions

[22]Similar comparisons for several other metals (vanadium, niobium, and molybdenum) also exhibit differences <5%.

[23]V. J. ORPHAN, N. C. RASMUSSEN, and T. L. HARPER, "Line and Continuum Gamma-Ray Yields from Thermal-Neutron Capture in 74 Elements," GA-10248, DASA-2500, Gulf General Atomic Report (1970).

TABLE I

Alternative Estimates of the $n,n' + n,2n$ Contribution to the Displacement Cross Sections of Iron and Tantalum*

Metal	E_n (MeV)	$\sigma_{n,n'}$	$\sigma_{n,2n}$	$F(E)\|_{n,n'+n,2n}$: Model ACS	Model 1-n	Model 2-n
Fe	12	1.17	0.046	2490	2480	2480
	13.5	0.90	0.33	2755	2692	2706
	15	0.56	0.59	2751	2680	2716
Ta	10	0.70	1.30	680	670	676
	12	0.28	1.72	798	796	799
	13.5	0.27	1.73	888	887	867
	15	0.35	1.70	998	1000	949

*All cross sections in b. Model designations are

ACS: $n,2n$ cross section added to n,n' cross section.
1-n: two neutrons treated as one in computing $F(E)|_{n,2n}$.
2-n: two neutrons treated sequentially; $F(E)|_{n,2n}$ computed from Eq. (21).

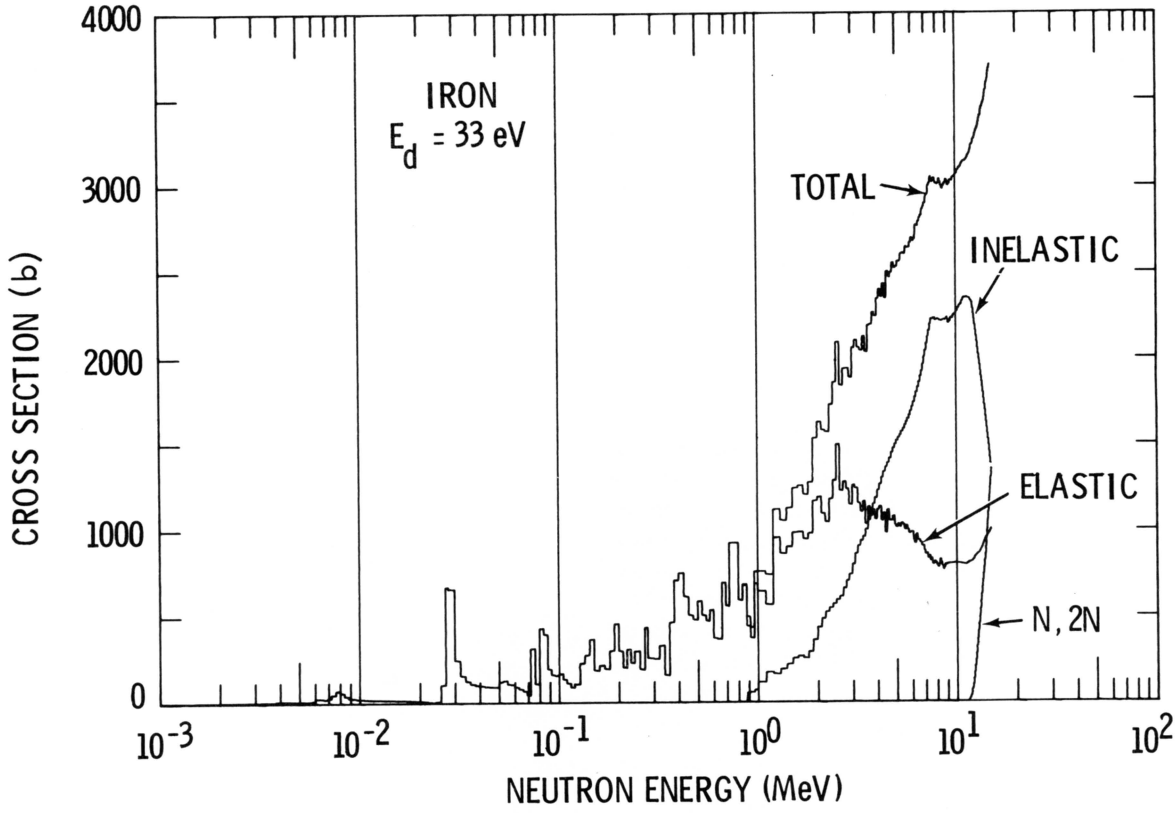

Fig. 3. The displacement cross section for iron.

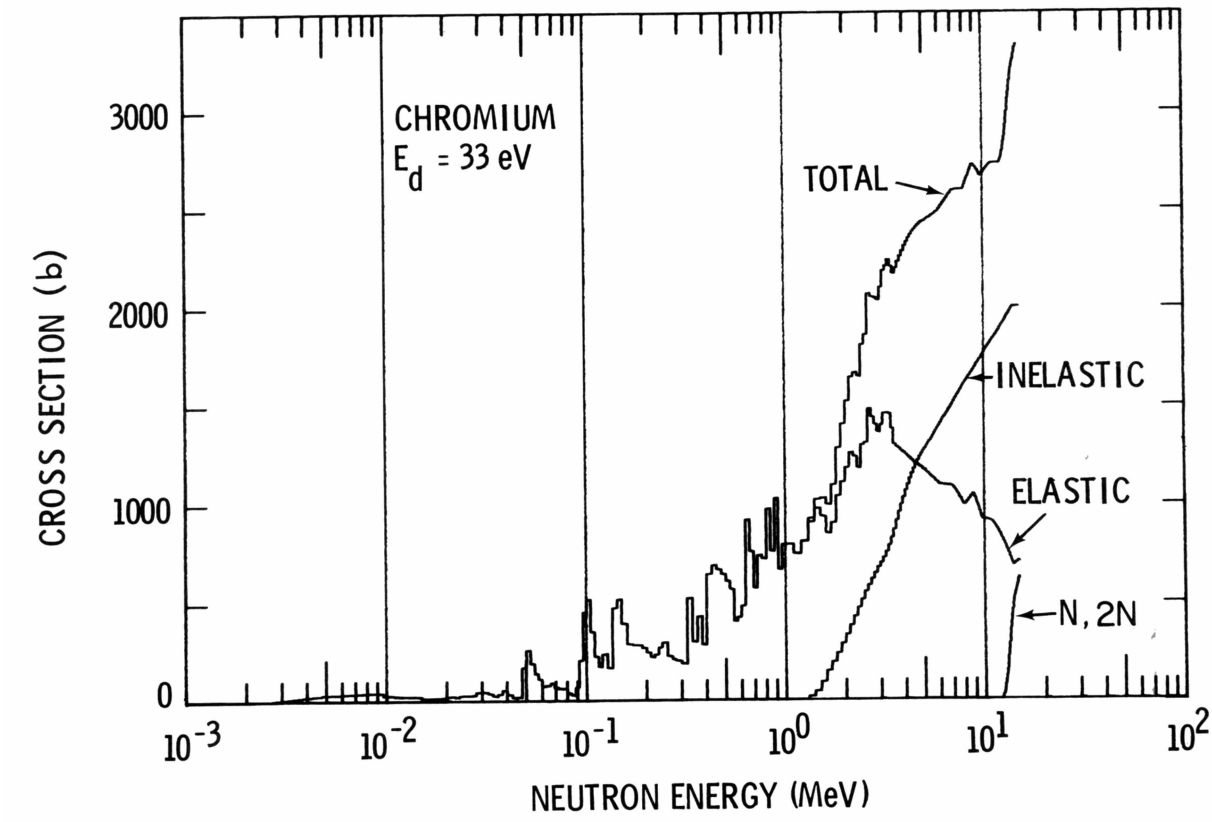

Fig. 4. The displacement cross section for chromium.

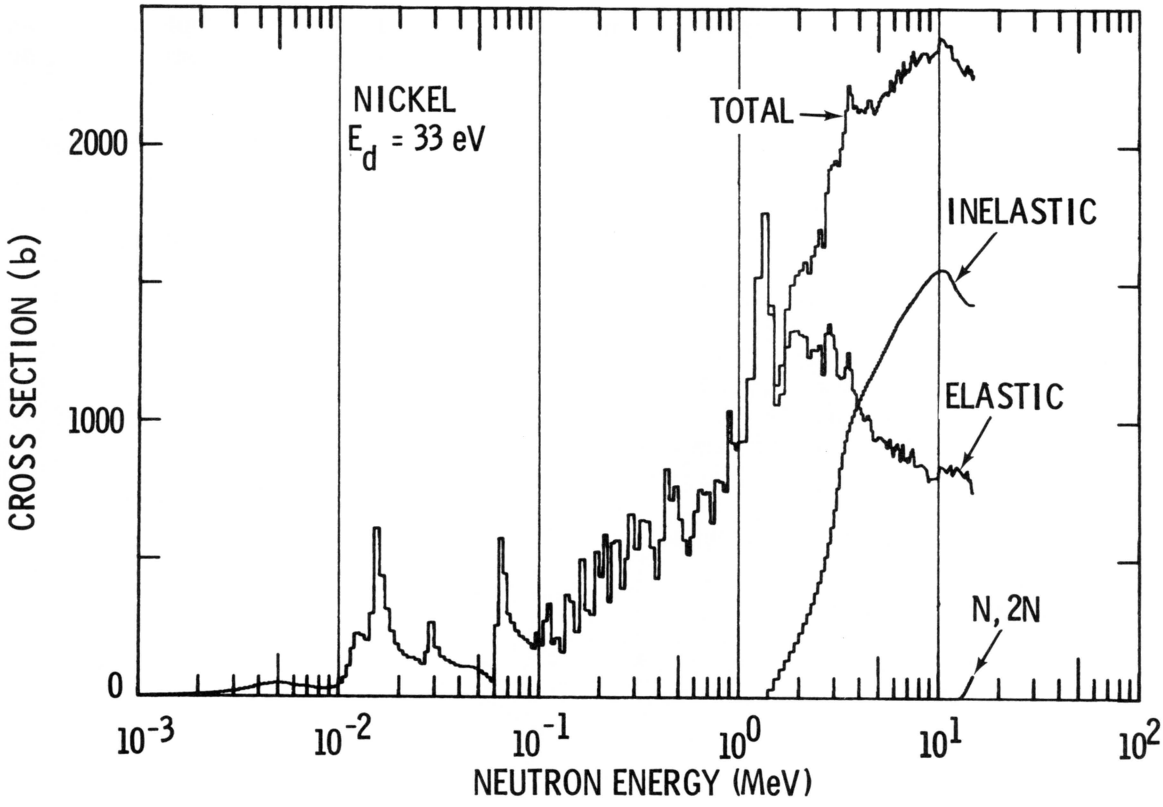

Fig. 5. The displacement cross section for nickel.

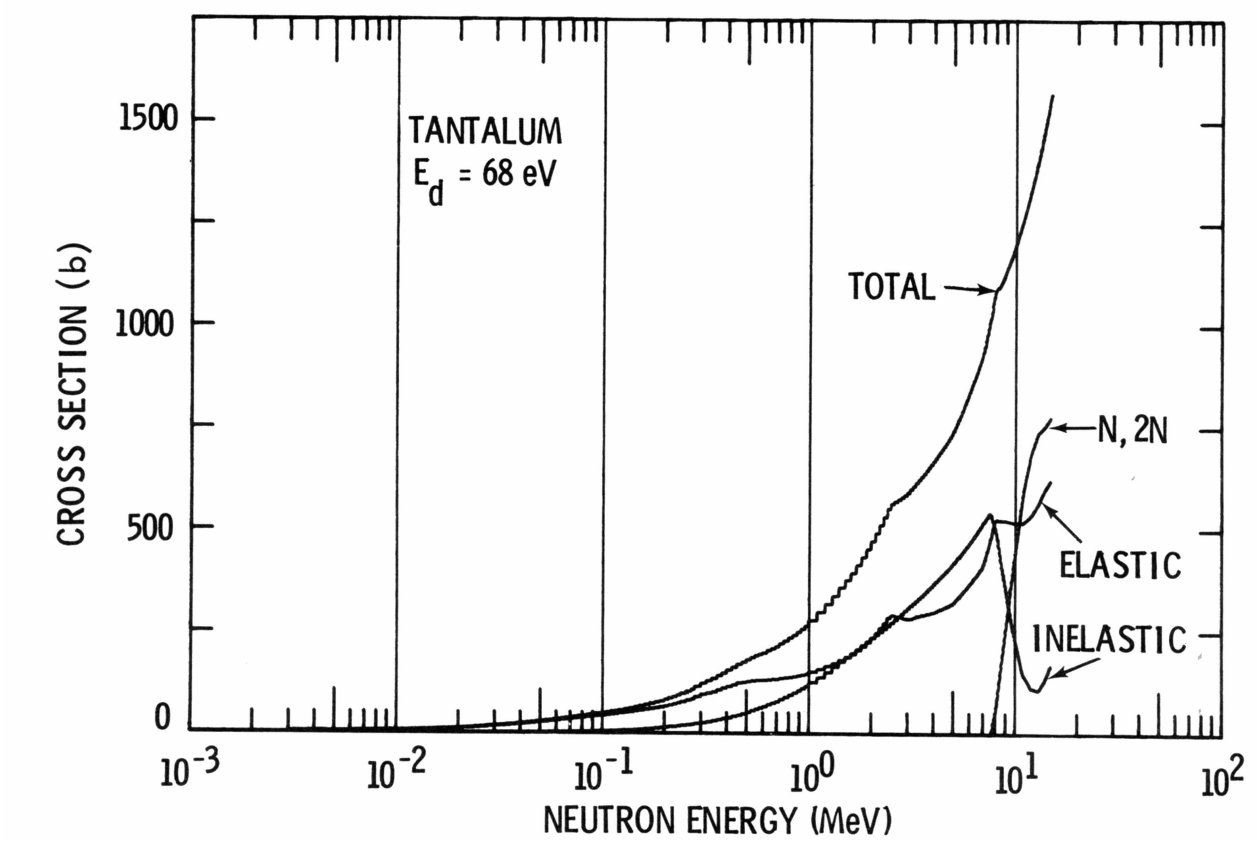

Fig. 6. The displacement cross section for tantalum.

for an 18% chromium, 10% nickel stainless steel are shown in Figs. 7 and 8; the latter figure includes the n,γ contribution. For convenience, the displacement cross section is presented in Table III for energies above 10^{-4} MeV. The groups correspond to 45 equal lethargy intervals per decade below 1 MeV and 0.1 MeV intervals above 1 MeV; no energy weighting has been employed. For energies less than 10^{-4} MeV, the displacement cross section varies as $E^{-1/2}$; its value at 0.025 eV is 20 b (see Table II).

Chabry and Genthon[24] calculated the energy deposited in the lattice per neutron for iron and tungsten from Lindhard's theory. Dividing their values for iron by $2E_d$ gives a displacement cross section in good agreement, in an averaged sense, with the present results.

It is of interest to compare the iron and stainless steel displacement cross sections. Above 4 MeV the constituent cross sections are ordered as Fe > Cr > Ni so that the stainless steel cross section is consistently less than that of iron. Between 1 and 4 MeV the difference between them is small and fluctuates in sign. Below 1 MeV the fluctuations are larger but the trend is for the stainless steel displacement cross section to exceed that of iron. Roughly speaking, the difference between the two is <20% above 0.03 MeV, <10% above 0.2 MeV, and <5% above 1 MeV. Clearly the displacement cross section for stainless steel is insensitive to the composition of the steel.

In Jenkins'[5] work on iron, he used the Kinchin-Pease model for the displacements produced per PKA, viz., $\beta = 1$ in Eq. (2) for $T \leq 56$ keV and $\nu(T) = \nu(56 \text{ keV})$ for $T > 56$ keV. Since $\beta < 1$ in the Lindhard model, the value of 33 eV assigned to E_d in the present work corresponds to a larger value in the Kinchin-Pease model. For example, to bring the displacement models into near coincidence for PKA energies of a few keV would require $E_d \sim 40$ eV. Since Jenkins used 25 eV,

[24] P. CHABRY and J. P. GENTHON, "Irradiation Damage from Pile Neutrons. Detailed Calculations on the Atomic Processes Involved. Program Source," CEA-N-1294 (in French), Commissariat a l'Energie Atomique, Saclay (1969).

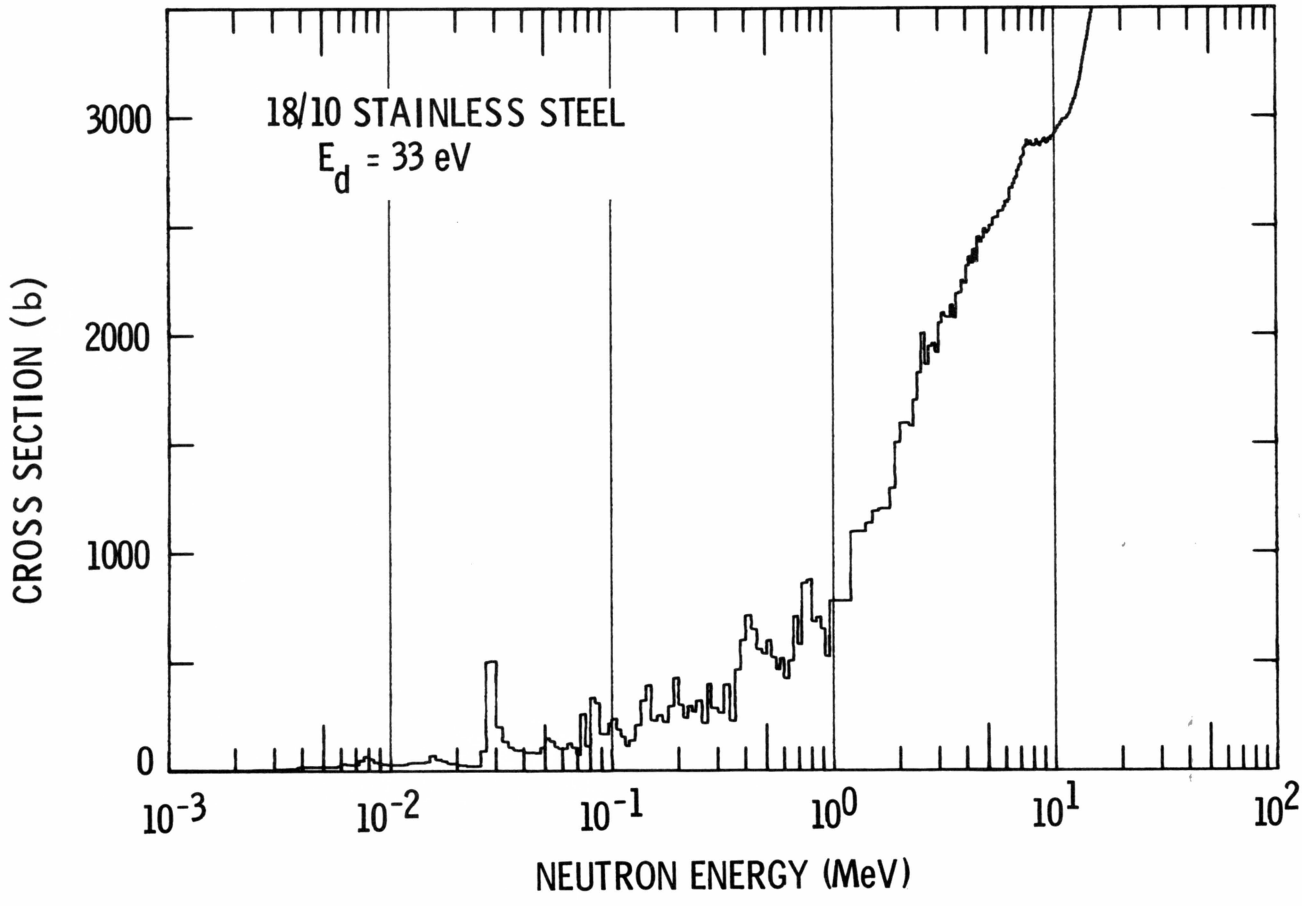

Fig. 7. The total displacement cross section for 18/10 stainless steel.

TABLE III

Displacement Cross Section (Disp/Atom-Fluence) for Stainless Steel Based on a Lindhard Model

Energy (MeV)	$F(E)$ (b)	Energy (MeV)	$F(E)$ (b)	Energy (MeV)	$F(E)$ (b)	Energy (MeV)	$F(E)$ (b)	Energy (MeV)	$F(E)$ (b)
1.000-04	3.260-01	1.050-04	3.201-01	1.100-04	3.143-01	1.150-04	3.084-01	1.200-04	3.011-01
1.275-04	2.923-01	1.350-04	2.836-01	1.425-04	2.762-01	1.500-04	2.690-01	1.600-04	2.617-01
1.700-04	2.544-01	1.800-04	2.470-01	1.900-04	2.397-01	2.000-04	2.341-01	2.100-04	2.302-01
2.200-04	2.263-01	2.300-04	2.224-01	2.400-04	2.175-01	2.550-04	2.116-01	2.700-04	2.067-01
2.800-04	2.009-01	3.000-04	1.940-01	3.200-04	1.905-01	3.400-04	1.870-01	3.600-04	1.835-01
3.800-04	1.800-01	4.000-04	1.746-01	4.250-04	1.698-01	4.500-04	1.651-01	4.750-04	1.742+00
5.000-04	1.827+00	5.250-04	1.913+00	5.500-04	1.997+00	5.750-04	2.080+00	6.000-04	2.171+00
6.300-04	2.275+00	6.600-04	2.374+00	6.900-04	2.471+00	7.200-04	2.582+00	7.600-04	2.701+00
8.000-04	2.819+00	8.400-04	2.934+00	8.800-04	3.042+00	9.200-04	3.154+00	9.600-04	3.240+00
1.000-03	3.410+00	1.050-03	3.673+00	1.100-03	1.732+01	1.150-03	1.740+01	1.200-03	4.205+00
1.275-03	4.393+00	1.350-03	4.610+00	1.425-03	4.826+00	1.500-03	5.089+00	1.600-03	5.527+00
1.700-03	5.641+00	1.800-03	5.890+00	1.900-03	6.132+00	2.000-03	6.427+00	2.100-03	6.788+00
2.200-03	7.159+00	2.300-03	7.576+00	2.400-03	8.035+00	2.550-03	8.677+00	2.700-03	9.242+00
2.800-03	9.949+00	3.000-03	1.098+01	3.200-03	1.212+01	3.400-03	1.337+01	3.600-03	1.497+01
3.800-03	1.865+01	4.000-03	1.883+01	4.250-03	1.873+01	4.500-03	2.078+01	4.750-03	2.398+01
5.000-03	2.519+01	5.250-03	2.439+01	5.500-03	2.416+01	5.750-03	2.531+01	6.000-03	3.234+01
6.300-03	3.054+01	6.600-03	2.910+01	6.900-03	3.375+01	7.200-03	4.735+01	7.600-03	6.514+01
8.000-03	5.669+01	8.400-03	4.242+01	8.800-03	3.404+01	9.200-03	2.974+01	9.600-03	2.661+01
1.000-02	2.557+01	1.050-02	2.622+01	1.100-02	2.906+01	1.150-02	3.428+01	1.200-02	3.957+01
1.275-02	3.852+01	1.350-02	3.606+01	1.425-02	4.461+01	1.500-02	7.259+01	1.600-02	5.561+01
1.700-02	4.404+01	1.800-02	3.557+01	1.900-02	3.057+01	2.000-02	2.755+01	2.100-02	2.444+01
2.200-02	2.127+01	2.300-02	2.170+01	2.400-02	2.573+01	2.550-02	9.415+01	2.700-02	5.034+02
2.800-02	5.064+02	3.000-02	2.010+02	3.200-02	1.334+02	3.400-02	1.081+02	3.600-02	9.757+01
3.800-02	9.473+01	4.000-02	8.673+01	4.250-02	8.163+01	4.500-02	7.966+01	4.750-02	1.087+02
5.000-02	1.484+02	5.250-02	1.375+02	5.500-02	1.113+02	5.750-02	1.014+02	6.000-02	1.054+02
6.300-02	1.274+02	6.600-02	1.089+02	6.900-02	7.481+01	7.200-02	2.642+02	7.600-02	1.117+02
8.000-02	3.392+02	8.400-02	3.091+02	8.800-02	1.698+02	9.200-02	1.715+02	9.600-02	2.207+02
1.000-01	2.375+02	1.050-01	1.891+02	1.100-01	1.560+02	1.150-01	1.157+02	1.200-01	1.422+02
1.275-01	2.129+02	1.350-01	3.253+02	1.425-01	3.949+02	1.500-01	2.293+02	1.600-01	2.570+02
1.700-01	2.237+02	1.800-01	2.988+02	1.900-01	4.298+02	2.000-01	2.998+02	2.100-01	2.427+02
2.200-01	2.994+02	2.300-01	2.694+02	2.400-01	3.241+02	2.550-01	2.175+02	2.700-01	4.011+02
2.800-01	2.848+02	3.000-01	2.672+02	3.200-01	3.979+02	3.400-01	2.290+02	3.600-01	4.672+02
3.800-01	6.029+02	4.000-01	7.144+02	4.250-01	6.471+02	4.500-01	5.549+02	4.750-01	5.369+02
5.000-01	5.981+02	5.250-01	5.214+02	5.500-01	4.622+02	5.750-01	5.187+02	6.000-01	4.212+02
6.300-01	5.084+02	6.600-01	7.111+02	6.900-01	5.774+02	7.200-01	8.632+02	7.600-01	8.732+02
8.000-01	6.823+02	8.400-01	7.044+02	8.800-01	6.480+02	9.200-01	5.226+02	9.600-01	7.801+02
1.000+00	7.827+02	1.100+00	7.805+02	1.200+00	1.099+03	1.300+00	1.096+03	1.400+00	1.133+03
1.500+00	1.190+03	1.600+00	1.200+03	1.700+00	1.202+03	1.800+00	1.298+03	1.900+00	1.508+03
2.000+00	1.598+03	2.100+00	1.591+03	2.200+00	1.583+03	2.300+00	1.701+03	2.400+00	1.828+03
2.500+00	2.010+03	2.600+00	1.861+03	2.700+00	1.949+03	2.800+00	1.957+03	2.900+00	1.917+03
3.000+00	2.057+03	3.100+00	2.101+03	3.200+00	2.080+03	3.300+00	2.079+03	3.400+00	2.138+03
3.500+00	2.074+03	3.600+00	2.191+03	3.700+00	2.196+03	3.800+00	2.251+03	3.900+00	2.238+03
4.000+00	2.318+03	4.100+00	2.359+03	4.200+00	2.329+03	4.300+00	2.392+03	4.400+00	2.333+03
4.500+00	2.451+03	4.600+00	2.423+03	4.700+00	2.447+03	4.800+00	2.488+03	4.900+00	2.468+03
5.000+00	2.477+03	5.100+00	2.504+03	5.200+00	2.505+03	5.300+00	2.537+03	5.400+00	2.543+03
5.500+00	2.538+03	5.600+00	2.570+03	5.700+00	2.568+03	5.800+00	2.571+03	5.900+00	2.591+03
6.000+00	2.615+03	6.100+00	2.606+03	6.200+00	2.619+03	6.300+00	2.676+03	6.400+00	2.671+03
6.500+00	2.696+03	6.600+00	2.717+03	6.700+00	2.723+03	6.800+00	2.754+03	6.900+00	2.766+03
7.000+00	2.779+03	7.100+00	2.813+03	7.200+00	2.821+03	7.300+00	2.861+03	7.400+00	2.869+03
7.500+00	2.895+03	7.600+00	2.868+03	7.700+00	2.878+03	7.800+00	2.886+03	7.900+00	2.869+03
8.000+00	2.864+03	8.100+00	2.865+03	8.200+00	2.874+03	8.300+00	2.896+03	8.400+00	2.884+03
8.500+00	2.872+03	8.600+00	2.864+03	8.700+00	2.880+03	8.800+00	2.888+03	8.900+00	2.894+03
9.000+00	2.903+03	9.100+00	2.892+03	9.200+00	2.879+03	9.300+00	2.884+03	9.400+00	2.898+03
9.500+00	2.900+03	9.600+00	2.894+03	9.700+00	2.906+03	9.800+00	2.909+03	9.900+00	2.914+03
1.000+01	2.925+03	1.010+01	2.933+03	1.020+01	2.944+03	1.030+01	2.950+03	1.040+01	2.958+03
1.050+01	2.957+03	1.060+01	2.964+03	1.070+01	2.974+03	1.080+01	2.979+03	1.090+01	2.987+03
1.100+01	2.991+03	1.110+01	2.990+03	1.120+01	2.988+03	1.130+01	2.994+03	1.140+01	2.998+03
1.150+01	3.006+03	1.160+01	3.010+03	1.170+01	3.015+03	1.180+01	3.021+03	1.190+01	3.035+03
1.200+01	3.051+03	1.210+01	3.055+03	1.220+01	3.064+03	1.230+01	3.077+03	1.240+01	3.084+03
1.250+01	3.094+03	1.260+01	3.109+03	1.270+01	3.121+03	1.280+01	3.132+03	1.290+01	3.144+03
1.300+01	3.161+03	1.310+01	3.180+03	1.320+01	3.200+03	1.330+01	3.217+03	1.340+01	3.238+03
1.350+01	3.256+03	1.360+01	3.273+03	1.370+01	3.288+03	1.380+01	3.304+03	1.390+01	3.319+03
1.400+01	3.334+03	1.410+01	3.351+03	1.420+01	3.369+03	1.430+01	3.390+03	1.440+01	3.409+03
1.450+01	3.426+03	1.460+01	3.441+03	1.470+01	3.457+03	1.480+01	3.475+03	1.490+01	3.493+03

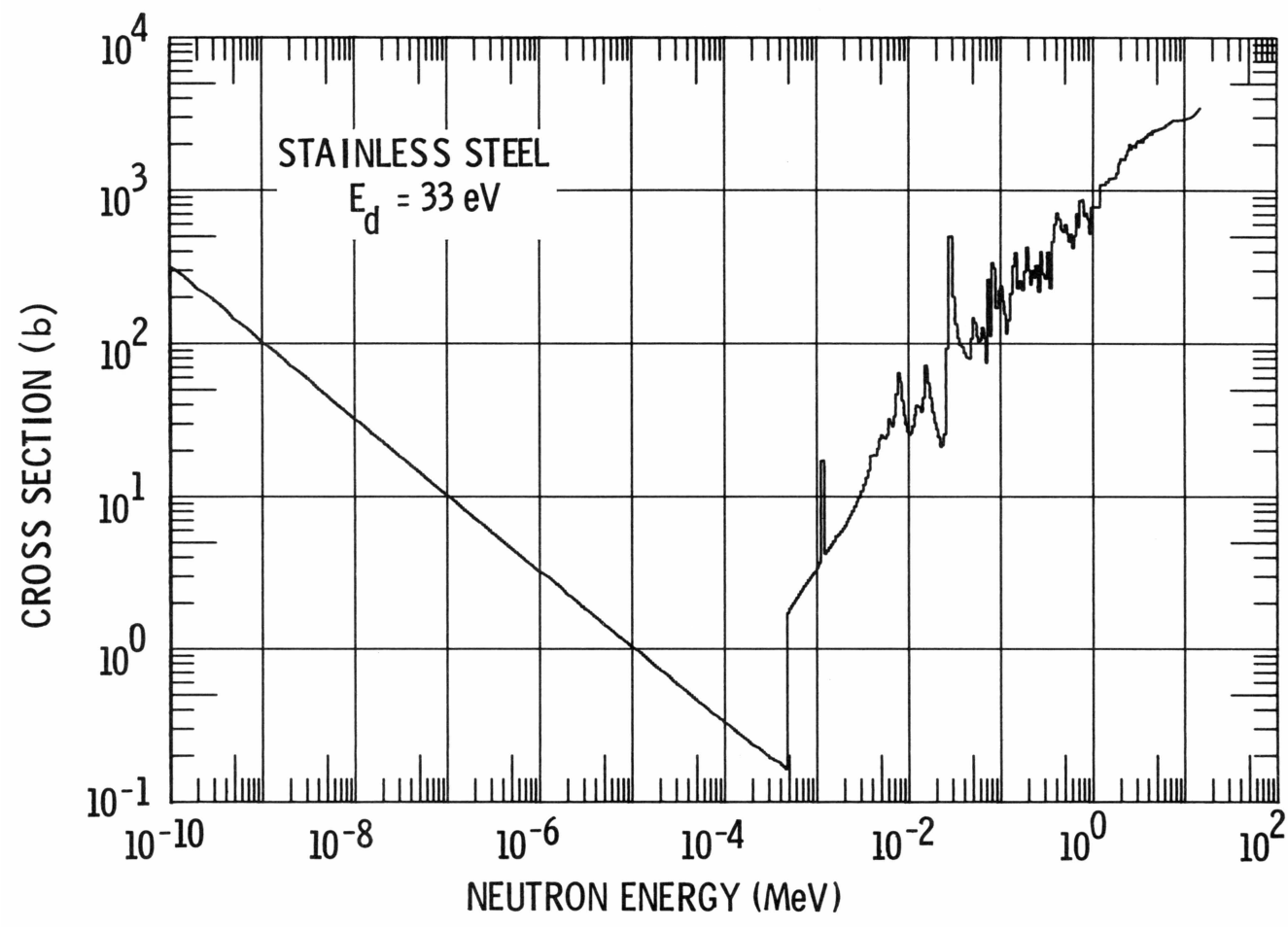

Fig. 8. The displacement cross section for 18/10 stainless steel including the n, γ contribution.

the upward displacement of his curve relative to the present results below ~1 MeV is due primarily to the difference in effective displacement energies and only secondarily to the difference in models (see Fig. 9). The relative decrease in Jenkins' cross section at higher energies is a consequence of the Kinchin-Pease assumption of a PKA ionization threshold (56 keV) above which all energy is dissipated in ionizing collisions that cause no displacements. In the Lindhard model, a significant, albeit decreasing, fraction of the energy is lost in displacement-producing collisions even at the highest PKA energies of interest. The two models are compared in Fig. 10. Note that, as pointed out above, the curves can be brought into near coincidence at low energies by a suitable choice of displacement energies.

In order to compare directly the Lindhard and Kinchin-Pease models, the displacement cross section for iron was recomputed using the latter model. A displacement energy of 40 eV was used to give agreement between the models at low energies—and hence agreement of both with Beeler (see Introduction). As can be seen in Fig. 11, the discrepancy becomes large above 3 MeV. A more quantitative comparison is facilitated by the group-averaged values of Table IV.

A common method of estimating displacement rates, because of its simplicity, is to use the Kinchin-Pease model and assume all energy is degraded in elastic, isotropic collisions. If the ionization threshold is designated by T_i and the scattering cross section by $\sigma(E)$, the displacement cross section can be expressed as

$$F(E)\Big|_{K\text{-}P/ISO} = \sigma(E)\gamma E/4\,E_d \qquad E \leq T_i/\gamma$$
$$= \sigma(E)\,T_i(2 - T_i/\gamma E)/4\,E_d \qquad E > T_i/\gamma\,.$$

This approximation is compared with the Lindhard theory result in Fig. 12 and Table IV. Again, a displacement energy of 40 eV and an ionization threshold of 56 keV were used.

In the low MeV region, the neglect of anisotropic scattering and the neglect of inelastic

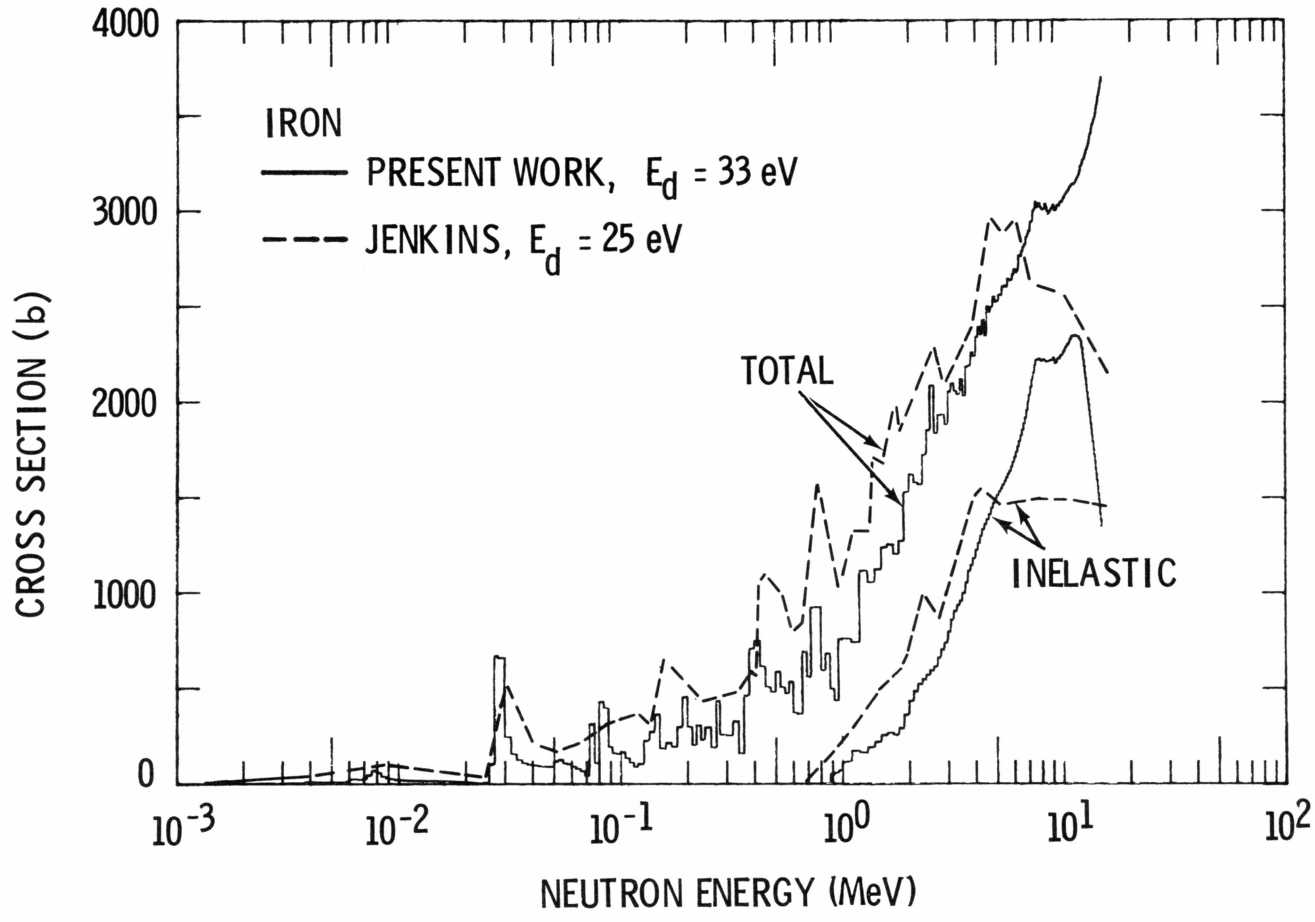

Fig. 9. The displacement cross section for iron compared with the results of Jenkins.

scattering partially compensate for one another. Hence this simple model yields a displacement cross section that does not differ significantly in the region below ~3 MeV from that computed with the more comprehensive Kinchin-Pease model of Fig. 11. Neither result is a good approximation of the Lindhard result above a few tenths MeV, except of course over a limited region (near 2 MeV) where the curves cross.

It is important that the limitations of the concept of a displacement cross section are recognized. Some investigators[8,24] have limited themselves to calculations of energy deposition, i.e., they have not attempted to convert deposition of energy to production of displacements. Energy deposition is a convenient measure of damaging irradiation dose if one material is irradiated at one temperature in various environments.[25] If different materials are to be compared (best done, perhaps, at equal homologous temperatures) the relative susceptibility to damage of the materials becomes important. This is one argument for introducing the displacement energies even though it is not clear what the proper effective values are. In view, however, of the multitude of variables that influence specific types of radiation damage, it can be questioned whether the conversion to displacement cross section is significant.

A better argument for providing displacement cross sections is that they serve as one starting point in the estimation of free and bound defect production rates in irradiated materials.[26] In this regard we should perhaps justify our neglect of energy-dependent processes that might negate the assumption [Eq. (1a)] that the number of displacements produced by a knock-on atom is proportional to the kinetic energy transferred to it.

[25]Implicit here is the assumption that the type of damage that concerns us is related to energy deposition (as opposed to effects of transmutation products, for example) and is generally initiated, therefore, by displacing atoms from normal lattice sites.

[26]D. G. DORAN, "Some Implications of the Computer Simulation of Displacement Cascades in Radiation Damage Modeling," HEDL-TME 71-181, Hanford Engineering Development Laboratory (1971).

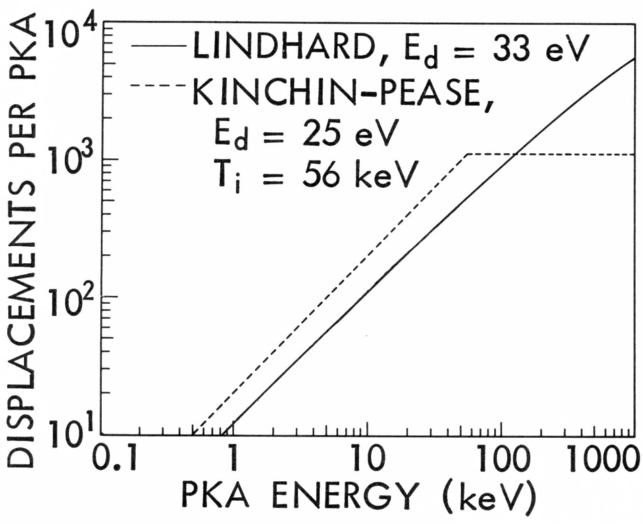

Fig. 10. A comparison of the Lindhard-based displacement model with the Kinchin-Pease model. The commonly used values, E_d = 25 eV and T_i = 56 keV, were employed in the latter.

Such processes include focusing, channeling, and interference between branches of a cascade. Appealing to computer simulation of displacement cascades, we find, as mentioned in the Introduction, that Beeler's results (extending to 20 keV) do indicate a departure from proportionality (attributed primarily to branch interference) but the effect is small. Torrens and Robinson have developed a new cascade simulation code—initial results with it show no departure from proportionality up to 100 keV.[13]

Of course, displacement production should not in general be equated with vacancy production. Because the present work is tied to Beeler's results[27] at low energy, "displacement" and "vacancy" are here synonymous at absolute zero for cascades produced in undamaged material. For practical irradiation temperatures, however, the degree of recombination is a function of temperature. Hence vacancy production depends on the temperature as well as the existing defect concentration in the material.[26,28]

SUMMARY AND CONCLUSIONS

Displacement cross sections have been calculated for stainless steel and for tantalum using Lindhard's model for the partition of energy during the slowing down of energetic atoms in solids. Aside from the question of the correctness of the model, the major uncertainty is in the scattering cross section at low energies and in the energy dependence of the anisotropy at high energies. New data are continually being generated and re-evaluated and the present treatment will be reviewed periodically.

It is clear that for spectra containing neutrons above ~1 MeV it is important to include the inelastic scattering contribution to the displacement cross section.

The $n,2n$ contribution has been considered in some detail because of possible materials applications in fusion reactors.

TABLE IV

Comparison of Displacement Cross Sections for Iron Based on Different Models

Neutron Energy (MeV) Lower Group Bound[a]	Displacement Cross Sections (b)		
	Lindhard[b] E_d = 33 eV	Kinchin-Pease[c] E_d = 40 eV T_i = 56 keV	Kinchin-Pease/ Isotropic[d] E_d = 40 eV T_i = 56 keV
6.065	2.955×10^3	1.580×10^3	1.278×10^3
3.679	2.488×10^3	1.630×10^3	1.451×10^3
2.231	1.967×10^3	1.472×10^3	1.428×10^3
1.353	1.345×10^3	1.231×10^3	1.260×10^3
0.821	7.963×10^2	8.798×10^2	9.216×10^2
0.498	6.146×10^2	7.242×10^2	7.925×10^2
0.302	4.881×10^2	5.558×10^2	5.800×10^2
0.183	2.947×10^2	3.272×10^2	3.355×10^2
0.111	2.121×10^2	2.309×10^2	2.296×10^2
0.067	2.015×10^2	2.141×10^2	2.091×10^2
0.041	9.938×10	1.056×10^2	1.030×10^2
0.025	2.377×10^2	2.525×10^2	2.458×10^2
0.015	1.020×10	1.084×10	1.054×10

[a]Groups correspond to lethargy increment of 0.5. Upper bound of first group is 10 MeV.

[b]Lindhard energy deposition model; includes treatment of anisotropic and inelastic neutron scattering.

[c]Kinchin-Pease energy deposition model; includes treatment of anisotropic and inelastic neutron scattering.

[d]Kinchin-Pease energy deposition model; neutron scattering assumed elastic and isotropic.

APPENDIX

Displacement Energies

The onset of damage production (change in electrical resistivity under electron bombardment) has been measured for iron and nickel by Lucasson and Walker.[29] For both iron and nickel,

[27]Beeler reported the number of vacancies remaining after a spontaneous recombination region was applied to an isolated cascade at absolute zero.

[28]D. G. DORAN and R. A. BURNETT, "Computer Simulation of the Short-Term Annealing of Displacement Cascades," *Interatomic Potentials and Simulation of Lattice Defects*, P. C. GEHLEN, J. R. BEELER, Jr., and R. I. JAFFEE, Eds., p. 403, Plenum Press, New York (1972).

[29]P. G. LUCASSON and R. M. WALKER, *Phys. Rev.*, 127, 485 (1962).

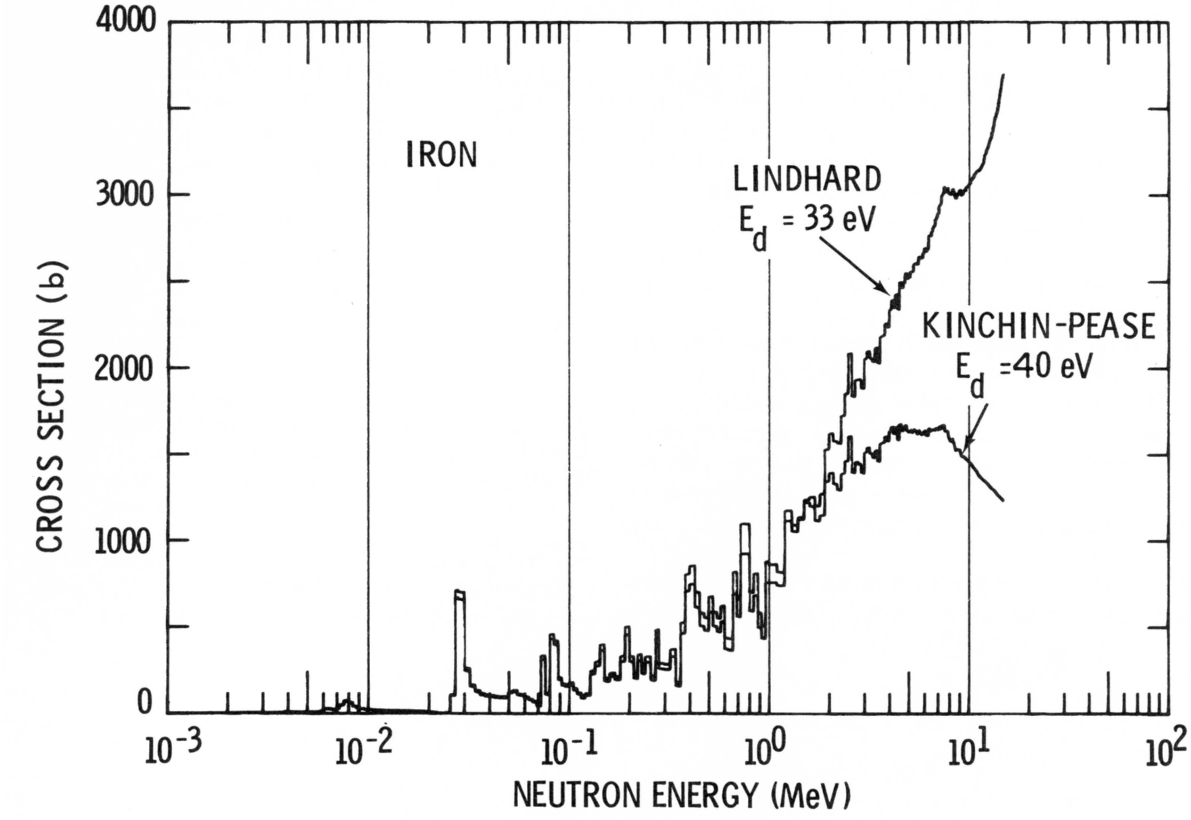

Fig. 11. A comparison of the Lindhard and Kinchin-Pease energy deposition models applied to iron (MAT 1124). Agreement at low energies was forced by the choice of E_d in the latter model.

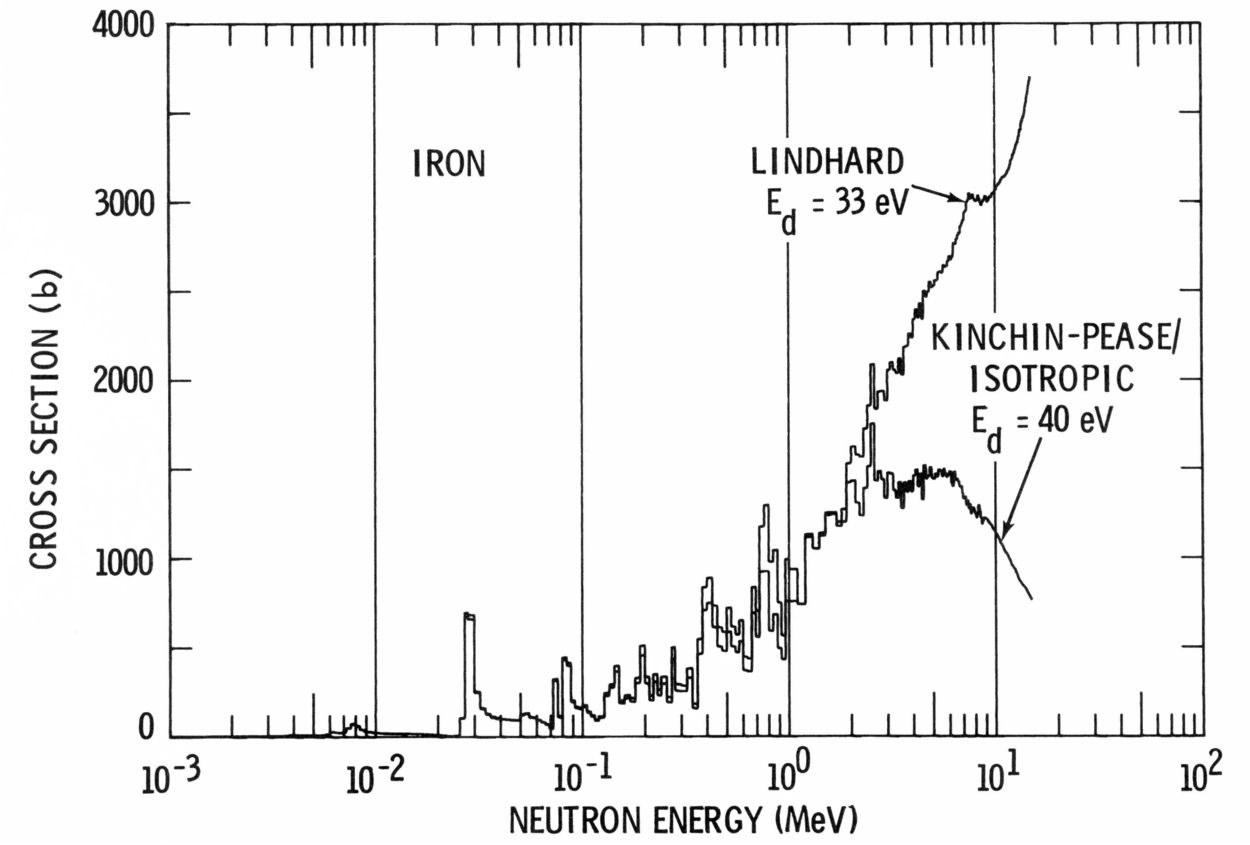

Fig. 12. A comparison of the Lindhard energy deposition model and the simple Kinchin-Pease model/isotropic scattering approach applied to iron. Agreement at low energies was forced by the choice of E_d in the latter model.

an effective displacement energy of ~24 eV was determined at ~20°K. This is the appropriate energy for a one-step displacement model, so the real threshold is somewhat lower. These values are lower limits for the quantity E_d of the present calculation for the following reason. The measurements were made by producing low concentrations of single defect pairs, whereas our concern is with displacement cascades produced by fast neutrons. In each of these cascades the damage is essentially saturated; hence significant annihilation takes place between "unrelated" pairs of defects and this increases the effective displacement energy. The procedure adopted here—choosing E_d to give agreement with Beeler's cascade simulations—is an attempt to compensate for this effect.

For tantalum, a threshold of 32 eV at 20°K was reported by Youngblood, Myhra, and DeFord.[30] The effective displacement energy for ejection in all possible directions should be considerably higher. In addition, the argument given above for iron and nickel applies here also.

ACKNOWLEDGMENTS

The author relied heavily on N. J. Graves for her programming and computational assistance and is indebted to B. D. Whitten for her careful preparation of the manuscript.

This paper is based on work performed under U.S. Atomic Energy Commission Contract AT(45-1)-2170. Hanford Engineering Development Laboratory is operated by Westinghouse Hanford Company, a subsidiary of Westinghouse Electric Corporation, for the U.S. Atomic Energy Commission, Richland, Washington.

[30]G. YOUNGBLOOD, S. MYHRA, and J. W. DeFORD, "Threshold Displacement Energy Measurements on Ta and Nb," COO-1494-7, University of Utah (1968).